RAPID COMMUNICATIONS

PHYSICAL REVIEW B VOLUME 46, NUMBER 11 15 SEPTEMBER 1992-I

Observation of normal-incidence intersubband absorption in *n*-type $Al_{0.09}Ga_{0.91}Sb$ quantum wells

E. R. Brown, S. J. Eglash, and K. A. McIntosh
Lincoln Laboratory, Massachusetts Institute of Technology, Lexington, Massachusetts 02173-9108
(Received 8 June 1992)

Normal-incidence intersubband absorption has been observed in *n*-type $Al_{0.09}Ga_{0.91}Sb$ quantum wells, as predicted by our previous calculation. The quantum wells were grown on (100)-GaSb and (100)-GaAs substrates and contain an electron sheet density of approximately 7×10^{11} cm^{-2}. The electrons occupy a two-dimensional *L*-point subband having ellipsoidal Fermi surfaces. For 7.0-nm-wide quantum wells, the absorption peak occurs at 870 cm^{-1} (11.5 μm), the peak fractional absorption per quantum well is 0.06%, and the full width at half maximum of the absorption profile is 30 meV. The measured absorption strength is within 12% of the theoretical calculation, which was based on the effective-mass method.

Since the observation of intersubband transitions in GaAs quantum wells,[1] there has been considerable interest in these transitions for infrared detection,[2] modulation,[3] and emission.[4] For *n*-type GaAs quantum wells in which the electrons occupy subbands with spherical Fermi surfaces, intersubband transitions occur only for the component of the optical electric field within the solid that is perpendicular to the plane of the quantum well. Therefore, plane-wave radiation propagating normal to the plane of the quantum well is not absorbed. The absence of normal-incidence absorption requires that *n*-GaAs intersubband detectors employ radiation coupling structures such as 45° facets in the substrate,[5] or sawtooth[6] or binary gratings[7] on the top surface. We recently predicted[8] that normal-incidence intersubband absorption would occur for *n*-type quantum wells in which the electrons occupy subbands with elliptical Fermi surfaces. In this paper we report strong normal-incidence intersubband absorption by *n*-type $Al_{0.09}Ga_{0.91}Sb$ in which electrons occupy such subbands. Normal-incidence absorption has been observed recently in *p*-type III-V,[9-11] *p*-Si,[11] and *n*-Si (Ref. 12) quantum wells, and we now report the observation of such absorption in *n*-type quantum wells made from III–V materials.

The polarization rules for intersubband transitions are explained by the following argument. In semiconductor quantum wells, the change in the electronic envelope function associated with a radiative intersubband transition occurs almost entirely along the direction normal to the plane of the well. The coupling between the envelope function and the optical electric field in the plane of the quantum well is expressed through the off-diagonal components of the reciprocal effective-mass tensor. In materials with spherical Fermi surfaces, the change in envelope function can be induced only by the normal component of the electric field because the off-diagonal components are always zero. However, in quantum wells made from ellipsoidal-Fermi-surface material and oriented so that the normal to the well is not a principal axis of the ellipsoids, the off-diagonal components can be of the same order of magnitude as (but necessarily less than) the largest diagonal component. Consequently, the change in envelope function can be induced by the component of electric field in the plane of the well, leading to a strong absorption of normal-incidence radiation.[8,13] Materials satisfying these requirements include (111)-Si and (100)-Ge,[13] (111)-$Al_xGa_{1-x}As$ with x near unity, and (100)-$Al_yGa_{1-y}Sb$ with $y\lesssim0.5$.[8]

For the present study three multiple-quantum-well (MQW) samples were grown by molecular beam epitaxy using solid sources of Al, Ga, As, and Sb, with GaTe providing Te for *n*-type doping. The growth rates were evaluated by means of reflection high-energy electron diffraction intensity oscillation measurements made during growth of the MQW samples. Each sample contains 100 $Al_{0.09}Ga_{0.91}Sb$ quantum wells confined by barriers of $AlAs_{0.08}Sb_{0.92}$ which is lattice matched to GaSb. Samples 1 and 2, which have nominal well widths of 7.0 and 6.4 nm, respectively, were grown on *n*-GaSb substrates. Sample 3, which has 7.0-nm quantum wells, was grown on a semi-insulating GaAs substrate to facilitate infrared measurements. The GaSb substrates exhibit much higher free-electron absorption because they are lightly *n* type. In all three samples the barriers are 20 nm thick. In sample 1 the barriers and quantum wells are doped uniformly with a nominal Te concentration of 2.5×10^{17} cm^{-3}. In samples 2 and 3 the barriers are undoped, while the quantum wells are doped to 1×10^{18} cm^{-3}. The outermost $AlAs_{0.08}Sb_{0.92}$ barriers were made 100 nm thick to confine electrons to the MQW region.

Infrared transmission measurements were made with a Fourier transform spectrometer over the wavelength range between about 4 and 16 μm. The three samples were measured in a single-pass configuration with light incident on the top surface both at Brewster's angle and at normal incidence. For Brewster's angle measurements the input radiation was polarized in the plane of incidence, so that no radiation was reflected at the air-semiconductor interfaces. In each measurement, the transmitted signal through the sample was divided by the transmitted signal through a bare substrate to correct for the background absorption. Multiple-pass interference fringes in the normal-incidence spectra arising from reflections within the epitaxial layers were subtracted numerically.

Figure 1 shows the single-pass spectra for sample 1 at room temperature. Transmission valleys are observed at about 870 cm^{-1} (11.5 μm) for Brewster's angle and 800 cm^{-1} (12.5 μm) for normal incidence. Both valleys cor-

 © 1992 The American Physical Society

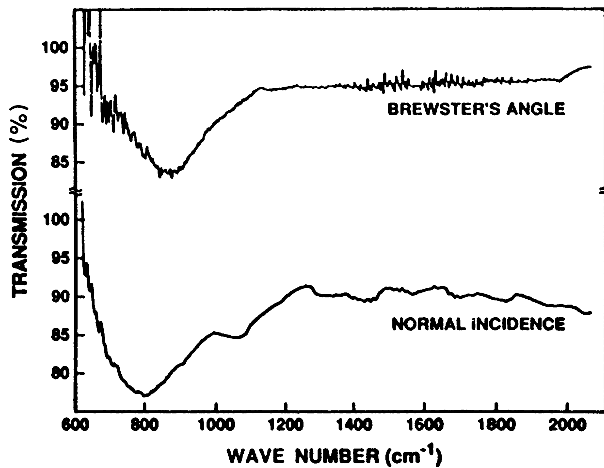

FIG. 1. Room-temperature transmission spectra for sample 1 (100 7.0-nm-wide $Al_{0.09}Ga_{0.91}Sb$ quantum wells on an *n*-GaSb substrate) in a single-pass configuration with the incident beam at Brewster's angle (75°) and at normal incidence.

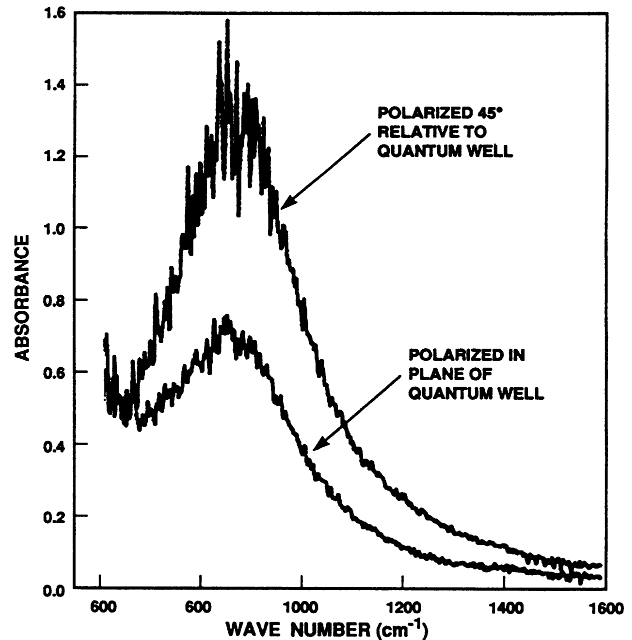

FIG. 2. Room-temperature absorbance spectra for sample 3 (100 7.0-nm-wide $Al_{0.09}Ga_{0.91}Sb$ quantum wells on a semi-insulating GaAs substrate) in multiple-pass configuration with the polarization either at 45° to the plane of the quantum wells or in the plane.

respond to a peak absorption of roughly 10% and a full width at half-maximum (FWHM) of approximately 200 cm^{-1}. The single-pass transmission spectra for sample 2 (not shown) display transmission minima at 1050 cm^{-1} (9.5 μm) for Brewster's angle and at a slightly lower wave number for normal incidence. The peak absorption strength and FWHM are practically the same as for sample 1. As discussed below, the 180-cm^{-1} shift in the transmission minima between samples 1 and 2 is consistent with the theoretical shift caused by the change in the well width. The single-pass transmission spectra for sample 3 are very similar to those for sample 1, indicating that the lattice mismatch between the epilayers and the GaAs substrate has little if any effect on the intersubband transition.

To obtain a more accurate characterization of the intersubband absorption in the $Al_{0.09}Ga_{0.91}Sb$ quantum wells, transmission measurements were made on sample 3 in a multiple-pass internal reflection (MIR) configuration. For this configuration, a small parallelepiped was cleaved from the wafer and 45° facets were lapped on the two ends. The incident beam was focused on one facet with its linear polarization either in the plane of the quantum wells or at 45° with respect to the plane, and the transmitted beam passed through the opposite facet. Shown in Fig. 2 are the absorbance spectra obtained by dividing the transmitted signal for each polarization by the corresponding transmitted signal through a GaAs MIR parallelepiped without the epilayers. Both spectra display well-defined absorption peaks superimposed on a background that slowly decreases with increasing wave number. The background is probably due to free-carrier absorption caused by electron scattering in the plane of the quantum wells. The in-plane absorption is the intersubband feature that has heretofore not been observed for any other *n*-type III–V material. After the background is subtracted, we obtain intersubband absorption profiles for the two incident polarizations that are centered at 890 cm^{-1} and have a FWHM of approximately 240 cm^{-1}. Because the MIR configuration provides far better resolution of the absorption profile than the single-pass configuration, the close agreement between the absorbance peak positions in the MIR and Brewster's-angle spectra suggests that the transmission minimum at normal incidence in Fig. 1 occurs at a wave number lower than the true value for intersubband absorption. We suspect that this shift results from imperfect numerical subtraction of the large interference fringes that occur at normal incidence.

To obtain a theoretical insight into the intersubband transitions, we have computed the low-lying energy levels in $Al_{0.09}Ga_{0.91}Sb$ quantum wells confined by AlSb barriers. Although the conduction-band minimum in bulk $Al_{0.09}Ga_{0.91}Sb$ occurs at the Γ point, in the quantum wells the Γ states are pushed above the L states by the stronger effect of spatial quantization on the lower-effective-mass Γ electrons. Therefore, the electronic ground state in the quantum wells is associated with the L point, occurring in the 6.4- and 7.0-nm wells at computed energies $E_1^{(L)}$ of 0.926 and 0.919 eV, respectively, relative to the valence band edge.[13] The next higher state is associated with the Γ point at energies $E_1^{(\Gamma)}$ of 0.939 and 0.928 eV for the two well widths. In spite of the close proximity of $E_1^{(L)}$ and $E_1^{(\Gamma)}$, the vast majority of electrons in both wells occupy the first L subband because of the much higher effective-mass density of states for electrons at the L point. Figure 3 compares the experimental results with the theoretical L-point intersubband energies $[E_2^{(L)}-E_1^{(L)}]$ calculated as a function of well width. Theory and experiment are in satisfactory agreement both for absolute wave number and for slope (i.e., the change in transition energy with

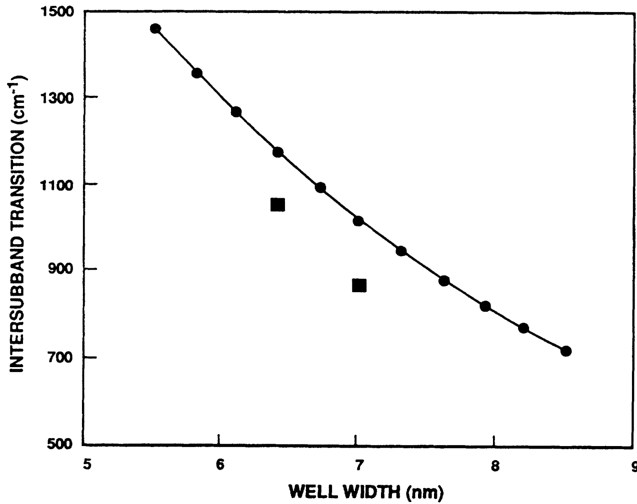

FIG. 3. Comparison of experimental (squares) and theoretical (circles) intersubband energies for samples 1 and 2 in single-pass configuration at Brewster's angle of incidence.

well width). In contrast, for a well width of 7.0 nm the intersubband transition between the first two Γ subbands would occur off scale at approximately 2100 cm^{-1}.[14] This analysis strongly supports the conclusion that the experimental absorption profile is the result of electron transitions from the first to the second L subbands.

The single-pass transmission spectra at Brewster's angle provide the best measure of the absolute intersubband absorption strength in these samples, since these spectra are not complicated by the multiple-pass interference that occurs at normal incidence in the single-pass configuration, or by the intensity cancellation that can occur near the surfaces of total internal reflection in the MIR configuration. Shown in Fig. 4 is the Brewster's-angle spectrum for sample 3 plotted in absorbance units. The maximum absorbance A_{max} is 0.036. This is related to the peak fractional absorption per well, ζ_p, by

$$A_{max} = -\log_{10}[(1-\zeta_p)^N] , \quad (1)$$

where $N(=100)$ is the number of quantum wells. Thus we find experimentally $\zeta_p = 8.1 \times 10^{-4}$.

We have previously derived[8] the following expression for ζ_p pertaining to a plane wave propagating through ellipsoidal-Fermi-surface quantum wells

$$\zeta_p = \frac{1024 e^2 \hbar \sigma w_{zz}}{27 \pi n c \Gamma} G(\theta,\phi) , \quad (2)$$

where σ is the electron sheet density per quantum well, w_{zz} is the diagonal element of the reciprocal effective-mass tensor along the normal to the quantum well, n is the optical refractive index, Γ is the FWHM of the absorption profile, and the other symbols have their conventional meanings. The quantity G is a geometrical factor that depends on both the orientation of the ellipsoids relative to the quantum well and the propagation vector of the plane wave as specified by the angles (θ,ϕ) relative to a polar axis normal to the quantum well. For L-point ellipsoidal subbands in (100)-oriented quantum wells and for radiation propagating at the angle θ and polarized in the plane of incidence, we found[8]

$$G = \frac{w_{zz}^{-2} \cos^2\theta}{9 m_{lt}^2} + \sin^2\theta . \quad (3)$$

The quantity m_{lt} is a characteristic mass related to the eccentricity of the ellipsoidal Fermi surfaces. Assuming that the $Al_{0.09}Ga_{0.91}Sb$ quantum wells have the same material properties as GaSb, we obtain $w_{zz}^{-1} = 0.12 m_0$, $m_{lt} = 0.086 m_0$, and $n = 3.8$ near a wavelength of 10 μm. We assume that σ is the product of the Te doping concentration (1×10^{18} cm^{-3}) and the well width, or $\sigma = 7 \times 10^{11}$ cm^{-2}. From the absorbance profile of sample 3 in the MIR configuration, $\Gamma = 240$ cm^{-1}. The angle θ is calculated from Snell's law and Brewster's formula as $\theta = \sin^{-1}[n^{-1}\sin(\tan^{-1}n)] = 14.7°$. Using all of these parameters, we find $G = 0.266$ and $\zeta_p = 9.1 \times 10^{-4}$, which is just 12% greater than the experimental value. Such a small discrepancy could be attributed to an overestimation of the sheet density in the first L subband. The benefit of the ellipsoidal-Fermi-surface quantum well is elucidated by noting that at this same angle of propagation, a spherical Fermi-surface well having the same material parameters (including w_{zz}) would exhibit $G = \sin^2\theta = 0.064$ and $\zeta_p = 2.2 \times 10^{-4}$.

We can also find the experimental ζ_p for normal-incidence radiation from the in-plane-polarized MIR spectrum in Fig. 2. After subtracting the background absorption, we find a peak absorbance of 0.48. This can be related to ζ_p as before, by assuming that the intensity in the MQW region is uniform and with Eq. (1) rewritten as $A_{max} = -\log_{10}[(1-\zeta_p)^{NP}]$, where P is the number of passes of the beam through the MQW structure. For our sample, $P \approx 15$, and we find $\zeta_p = 6.3 \times 10^{-4}$. The theoretical ζ_p is found from Eq. (2) with G given by $w_{zz}^{-2}/9m_{lt}^2$, which applies to incident radiation polarized in the plane

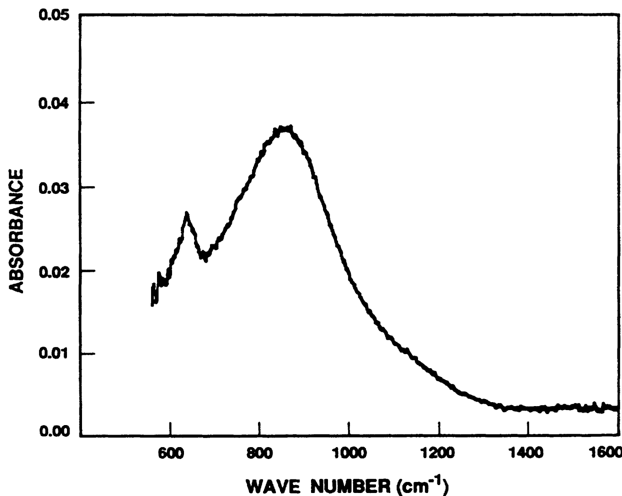

FIG. 4. Room-temperature absorbance spectrum for sample 3 at Brewster's angle. The small peak near 630 cm^{-1} is thought to be caused by third-order phonon absorption in the $AlAs_{0.08}Sb_{0.92}$ barrier material.

of the quantum well.[8] The value of ζ_p is thus 7.4×10^{-4}, in good agreement with experiment.

In summary, we have observed normal-incidence absorption caused by intersubband transitions in n-type III–V quantum wells. Our $Al_{0.09}Ga_{0.91}Sb$ quantum wells are narrow enough that the electron ground state is associated with the L point. The observed transition energies are consistent with the theoretical separation between the first and second L-point envelope states in the wells. The most reliable value of the absorption strength, which was determined from measurements at Brewster's angle, is within 12% of the theoretical prediction for intersubband transitions in ellipsoidal-Fermi-surface quantum wells. The strong absorption at normal incidence is expected to lead to improved performance of intersubband optical devices operating in the 8- to 12-μm band.

The authors thank A. J. Strauss, R. A. Murphy, and D. L. Spears for programmatic support and useful comments on the manuscript, G. W. Turner for collaboration on the photoluminescence characterization of $Al_xGa_{1-x}Sb$ materials, and J. V. Pantano, M. P. Walsh, D. R. Calawa, J. W. Chludzinski, and L. Krohn for technical support. This work was sponsored by the Defense Advanced Research Projects Agency.

---

[1]L. C. West and S. J. Eglash, Appl. Phys. Lett. **46**, 1156 (1985).

[2]B. F. Levine, C. G. Bethea, G. Hasnain, J. Walker, and R. J. Malik, Appl. Phys. Lett. **53**, 296 (1988).

[3]R. P. G. Karunasiri, Y. J. Mii, and K. L. Wang, IEEE Electron. Device Lett. **11**, 227 (1990).

[4]M. Helm, P. England, E. Colas, F. DeRosa, and S. J. Allen, Jr., Surf. Sci. **228**, 120 (1990).

[5]B. F. Levine, C. G. Bethea, K. K. Choi, J. Walker, and R. J. Malik, Appl. Phys. Lett. **53**, 231 (1988).

[6]G. Hasnain, B. F. Levine, C. G. Bethea, R. A. Logan, J. Walker, and R. J. Malik, Appl. Phys. Lett. **54**, 2515 (1989).

[7]J. Y. Andersson and L. Lundqvist, Appl. Phys. Lett. **59**, 857 (1991).

[8]E. R. Brown and S. J. Eglash, Phys. Rev. B **41**, 7559 (1990).

[9]B. F. Levine, S. D. Gunapala, J. M. Kuo, S. S. Pei, and S. Hui, Appl. Phys. Lett. **59**, 1864 (1991).

[10]J. Katz, Y. Zhang, and W. I. Wang, Electron. Lett. **28**, 932 (1992).

[11]R. P. G. Karunasiri, J. S. Park, and K. L. Wang, Appl. Phys. Lett. **59**, 2588 (1991).

[12]C. Lee and K. L. Wang, Appl. Phys. Lett. **60**, 2264 (1992).

[13]C. L. Yang, D. S. Pan, and R. Somoano, J. Appl. Phys. **65**, 3253 (1989).

[14]The electrons in the L and Γ subbands of the quantum well are assumed to be confined by the L- and Γ-point band edges, respectively, of the AlAsSb barriers. The L and Γ barrier heights are assumed to be 65% of the difference in L and Γ band gaps, respectively, between AlSb and $Al_{0.09}Ga_{0.91}Sb$.